Carbohydrate Polymers 83 (2011) 122–129

Contents lists available at ScienceDirect

Carbohydrate Polymers

journal homepage: www.elsevier.com/locate/carbpol

Preparation and characterization of cellulose nanowhiskers from cotton fibres by controlled microbial hydrolysis

Prasad Satyamurthy, Prateek Jain, Rudrapatna H. Balasubramanya, Nadanathangam Vigneshwaran*

Nanotechnology Research Group, Chemical and Biochemical Processing Division, Central Institute for Research on Cotton Technology, Adenwala Road, Matunga, Mumbai 400 019, India

ARTICLE INFO

Article history:
Received 1 April 2010
Received in revised form 15 July 2010
Accepted 15 July 2010
Available online 21 July 2010

Keywords:
Cellulase
Cellulose nanowhiskers
Chiral nematic phase
Trichoderma reesei
Microcrystalline cellulose
Nanomaterials

ABSTRACT

The cellulolytic fungus *Trichoderma reesei* was used to prepare cellulose nanowhiskers (CNW) by controlled hydrolysis of microcrystalline cellulose (MCC). The penetration of fungus into the ordered regions of MCC resulted in reduction (10%) of its crystallinity. The zeta potential of fungal hydrolyzed CNW was similar to that of native MCC while that of CNW prepared by acid hydrolysis was five times higher due to its surface sulfation. Also, fungal hydrolyzed CNW resulted in monodomain structure under polarized light microscopy (PLM) while it was polydomain for that of acid hydrolyzed CNW. Atomic force microscopic (AFM) analysis confirmed the preferential orientation (anisotropy) of CNW on drying. Preparation of CNW by concentrated sulfuric acid hydrolysis process is energy intensive, environmentally hazardous and the surface of CNW is chemically modified (sulfated). But fungal hydrolysis resulted in CNW without any surface modification and such nanostructures show promise for applications in eco-friendly composites and pharmaceuticals.

1. Introduction

Cellulose is a homopolymer of β-1,4-D-glucose molecules linked in a linear chain. Among various sources like plants, algae, marine creatures and bacteria, cotton contains the highest percentage of cellulose (>95%). The single cotton fibre (thickness: 20–30 μm) consists of superfine fibrils having diameter in the range of nanometer. The nano-architecture of the cellulose promotes isolation of nanowhiskers and nanofibrils. Cellulose from cotton fibres may be hydrolyzed using enzymes to produce glucose, which can be used for the production of ethanol (Olsson & Hahn-Hagerdahl, 1996), organic acids (Luo, Xia, Lin, & Cen, 1997), and other chemicals (Cao, Xia, Gong, & Tsao, 1997). Because of zero-toxicity, good hygroscopicity and chemical inactivity, high-quality microcrystalline cellulose (MCC) produced from cotton cellulose is used as an excipient for tablets, gentle filler in cosmetic creams, and as an additive to dietary food (Kleinebudde, Jumaa, & El Saleh, 2000). The CNW, also called as nanocrystalline cellulose, cellulose crystallites or crystals in the literature, are produced by concentrated sulfuric acid hydrolysis of MCC whereby the presence of amorphous region is completely hydrolyzed to yield highly crystalline CNW. These CNW have received increasing attention due to their extraordinary mechanical properties such as high Young's modulus and tensile strength (Sturcov, Davies, & Eichhorn, 2005). The Young's modulus of CNW is as high as 134 GPa while the tensile strength of the crystal structure was estimated in the range of 0.8–10 GPa (Lee, Mohan, Kang, Doh, Lee, & Han; Nishino, Takano, & Nakamae, 1995). The hydrolyzing agent, sulfuric acid introduces bulky ester groups onto the hydroxyl groups and stabilizing the CNW in solution by preventing its agglomeration (Araki, Wada, Kuga, & Okana, 1998). However, the use of sulfuric acid has a number of important drawbacks such as corrosivity, surface modification of cellulose and environmental incompatibility. Similarly, the sono-chemical assisted hydrolysis of cellulosic materials for the production of CNW (Filson & Dawson-Andoh, 2009) is highly energy intensive. The isolation or disintegration of MCC without severe degradation and at reasonable costs is still difficult.

The filamentous fungus *Trichoderma reesei* (anamorph of *Hypocrea jecorina*) is one of the most efficient producers of extra cellular cellulase enzyme. Cellulases are produced as multi component enzyme system comprised usually of three components that act synergistically in the hydrolysis of cellulose; endoglucanases (EC 3.2.1.4), cellobiohydrolase (EC 3.2.1.91) and cellobiase (β-glucosidase, EC 3.2.1.91). The extracellular cellulolytic system of *T. reesei* is composed of 60–80% cellobiohydrolases, 20–36% of endoglucanases and 1% of β-glucosidases (Zaldivr, Velasquez, Contreras, & Perez, 2001). The first two components act directly on cellulose yielding mainly cellobiose, cellotriose or cellotetraose as the reaction products. The cellobiose is then hydrolyzed to glucose by cellobiase. Though endoglucanases and cellobiohydrolases

* Corresponding author. Tel.: +91 22 24127273; fax: +91 22 24130835.
E-mail address: nvw75@yahoo.com (N. Vigneshwaran).

0144-8617/$ – see front matter © 2010 Elsevier Ltd. All rights reserved.
doi:10.1016/j.carbpol.2010.07.029

degrade soluble cellodextrins and amorphous cellulose, cellobiohydrolases degrade crystalline cellulose more efficiently (Bhat & Bhat, 1997). The oligosaccharides formed during the cellulose hydrolysis are believed to play important roles in the natural cellulase induction; so solid cellulose itself is often used as both the substrate and the source of inducers in the fermentation processes for cellulase production.

Cellulose and its derivatives are found to form chiral nematic phases and this ordered molecular structure was preserved in solid films by slow evaporation of the liquid (Charlet & Gray, 1987). These ordered suspensions solidify on evaporation of the water to give helicoidal structures resembling those in various biological skeletal materials. These liquid crystalline characteristics are attributed to the presence of parallel alignments of the anisotropic crystallites (nematic order).

Earlier work showed a significant reduction in energy consumption during refining process when the feed material (cellulose) is subjected to fungal pretreatment (Janardhnan & Sain, 2006). The energy consumption in refining process was very high due to the predominating hydrogen bonding between the cellulose microfibrils. This interfibrillar hydrogen bonding energy (~20 MJ/kg mol) has to be overcome in order to hydrolyze the cellulose. As a biological catalyst, action of microbial enzymes reduces the energy requirement for cellulose hydrolysis. Recently, an attempt was made to characterize the residues extracted after enzymatic hydrolysis of MCC derived from an alga (*Cladophora* sp.) that showed the formation of nano-ordered short elements containing cellulose I_β crystalline domains. But, the process was very slow and required continuous replenishment of enzymes to reach 80% hydrolysis of MCC (Hayashi, Kondo, & Ishihara, 2005). Therefore, the present study was attempted to produce CNW by controlled hydrolysis of MCC using the fungus *T. reesei* under submerged fermentation process. The CNW obtained was characterized by DLS particle size analyzer, XRD, polarized light microscopy and AFM.

2. Experimental

2.1. Preparation of cellulose substrates

The MCC was prepared from the cotton fibres (short staple cotton variety: *Bengal desi*) by conventional hydrochloric acid hydrolysis (4 N HCl). This resulted in MCC with wide size distribution in the micrometer range. To have uniform size distribution, the MCC was sieved through various sieves and the size range of 45–53 μm was selected for further work.

2.2. Microbial hydrolysis of MCC

The 24 h inoculum of the fungus *T. reesei* (ATCC 13631) was prepared in potato dextrose broth by inoculation of spore suspension (~3×10^6 spores/ml). The optimized concentration (5.0%) of inoculum was added in Mandel's medium having MCC as the sole carbon source in 250 ml conical flask at 25 °C/30 °C under shaking condition (150 rpm). After fermentation, the broth was subjected to differential relative centrifugal forces (Bai, Holbery, & Li, 2009) to optimize the sedimentation of all particles of size more than 1 μm. The resultant supernatant was filtered through 100 kDa ultrafiltration membrane by vacuum suction and the CNW trapped on the surface of membrane was removed with a jet of ultrapure water and freeze dried (Vigneshwaran & Kathe, 2009) for further analysis. The cellulose content was determined by using the method as described by Updegraff (1969). Yield was calculated as the percent of cellulose content to that of initial MCC concentration. For comparison, CNW was prepared by conventional process using 64 wt.% of sulfuric acid hydrolysis of MCC at 35 °C for 1 h. The acid hydrolyzed sample was neutralized with excess of water and washed with water by repeated centrifugation till the pH was neutralized and freeze dried.

2.3. Enzyme analysis

The cellulase activity of the culture filtrate was determined by using the assay procedure described elsewhere (Ghose, 1987). The cellulase activity was measured by filter paper assay (FPA), CMC assay and ρNPG assay. The reducing sugars were measured for FPA and CMC assay by Nelson Somogyi method (Nelson, 1944) while ρ-nitrophenyl glucose was measured for ρNPG assay (Barbagallo et al., 2004). The activity is expressed as IU/ml of filtrate which corresponds to one μmol of glucose released per minute per ml. For determination of biomass concentration, the glucosamine content was used as an indirect method (Abd-Aziz et al., 2008) using the colorimetric method as described in the literature (Elson & Morgan, 1933). Electrophoresis of concentrated enzyme was carried out to determine the various enzyme components based on their molecular weights (Weber & Osborn, 1969). The fermented broth was filtered through G3 silica crucible to remove the fungal biomass and the proteins in filtrate were precipitated by saturated ammonium sulfate precipitation. The precipitated proteins were dissolved in acetate buffer of pH 4.8 and used for SDS-PAGE. SDS-PAGE was done in the vertical electrophoresis setup with 7.5% gels along with the protein marker (Protein Mixture IV, Merck Biosciences). Degree of polymerization (DP) was measured viscosimetrically in copper ethylenediamine solution and the obtained intrinsic viscosities were converted into the respective values of DP by Eq. (1) (Grobe, 1989).

$$\mathrm{DP} = \left[\frac{2000\eta_{\mathrm{spec}}}{c(1+0.29\eta_{\mathrm{spec}})}\right] \quad (1)$$

where, $\eta_{\mathrm{spec}} = (\eta/\eta_0 - 1)$; η_{spec} is specific viscosity; η/η_0 is relative viscosity and c is concentration in g/l.

2.4. Particle size and zeta potential measurements

The particle size distribution and zeta potential of CNW in suspension were measured using Nicomp™ 380 ZLS size analyzer. The instrument employs a design, which permits both multi-angle particle size analysis by DLS and low-angle zeta potential analysis by electrophoretic light scattering (ELS). Size calibration was carried out using 90 nm size polystyrene latex spheres and zeta potential calibration by using 491 nm polystyrene latex spheres. The size distribution was obtained based on the dynamic light scattering and autocorrelation principle. The mean diameter of the particles was calculated from their Brownian motion via the Stokes–Einstein equation. For this, HeNe laser (632.8 nm) was used and the scattering intensity was analyzed by Avalanche photodiode detector at 90° orientation.

2.5. X-ray diffraction analysis

Wide angle X-ray diffraction patterns of MCC and CNW were obtained using a Philips® PW 1710 X-ray diffractometer with nickel filtered Cu Kα (λ = 1.54 Å) radiation and analyzed using automatic powder diffraction (APD) software. The diffracted intensities were recorded from 10° to 80° 2θ angles. Both MCC and CNW samples were prepared by freeze drying the aqueous suspension. The periodical distances (d) of the main peaks were calculated according to Bragg's equation ($\lambda = 2d\sin\theta$). Crystallinity of the sample was determined by using Eq. (2).

$$\%\mathrm{Crystallinity} = \left[\frac{I_c - I_a}{I_c}\right] \times 100 \quad (2)$$

where, I_c is peak intensity of crystal plane (0 0 2) and I_a is peak intensity of amorphous phase ($2\theta = 18$). The crystallite size was calculated using the Scherrer equation (3).

$$L_{h,k,l} = \frac{K\lambda}{\beta \cos\theta} \quad (3)$$

where, $K = 0.94$ (Revol, Dietrich, & Goring, 1987), $\lambda = 1.5418$ Å, θ is diffraction angle corresponding to (0 0 2) crystal plane and β is the full width at half maximum of the peak angle of (0 0 2) crystal plane.

2.6. Microscopic analysis

For PLM analysis, a drop of CNW suspension was deposited on a strain free glass slide and air-dried. The photomicrographs were recorded by keeping the sample in between crossed polarizers using a polarized light microscope (Leica™). The AFM analysis was carried out using a diInnova AFM (Veeco, Santa Barbara, CA, US) equipped with a 90 μm scanner. A drop of CNW suspension was deposited onto a freshly cleaved mica surface and air-dried. All images were obtained using tapping mode in air at room temperature. The silicon nitride cantilever with a spring constant of 40 N m^{-1} was used. The scan rate of 1.0 Hz and 512 lines per 5 μm was used to optimum contrast. No filtering was used during scanning.

2.7. FTIR analysis

For Fourier Transform Infrared (FTIR) analysis, the freeze dried CNW was diluted with potassium bromide in the ratio of 1:100 and made into a pellet. This pellet was analyzed using an IRPrestige-21® FTIR in transmission mode. For comparison, pristine cotton cellulose was used for analysis. The spectra recorded were the average of 100 scans and the contribution of background was accounted for during analysis.

3. Results and discussion

The enzymatic hydrolysis of cellulose, particularly hydrogen-bonded and ordered crystalline regions of MCC, is a very complex process. As the MCC is insoluble, the cellulase enzyme could not diffuse into the structural features of the substrate (Hayashi, Sugiyama, Okano, & Ishihara, 1997). So, hydrolysis of MCC by enzyme will be a slower process as it has to proceed from surface to innermost. Among the two major types of cellulose (algal–bacterial type rich in cellulose I_α crystalline region and cotton–ramie type rich in cellulose I_β), algal–bacterial type is highly susceptible to cellulase enzyme. The cotton cellulose is recalcitrant due to the dominance of cellulose I_β structure. Earlier research in our laboratory on enzymatic hydrolysis of cotton cellulose by continuous and repeated process resulted in the formation of nano-sized cellulose particles of size ranging from 90 to 300 and 30 to 50 nm, respectively (Paralikar & Bhatawdekar, 1983). But, the major problem faced was the loss in enzyme activity and low rate of hydrolysis. So, instead of enzymatic hydrolysis, microbial hydrolysis was chosen for the preparation of CNW. Fungal hydrolysis accelerates the process of MCC hydrolysis by mycelia penetration. Among the two major extra cellular cellulase producing fungi, *T. reesei* and *Aspergillus* species, *T. reesei* was chosen due to their low level of β-glucosidase enzyme; since our aim was to avoid complete hydrolysis to monomer (glucose). The use of MCC in fermentation process poses a problem of nutrient availability due to its insolubility. The exoglucanase component of cellulase enzyme is the active participant in hydrolyzing the crystalline region of MCC. So, we have optimized the process condition for increased production of exoglucanase by the *T. reesei*. This fungus, when grown using synthetic medium at 25 °C showed the highest exoglucanse activity than any other conditions we have tried.

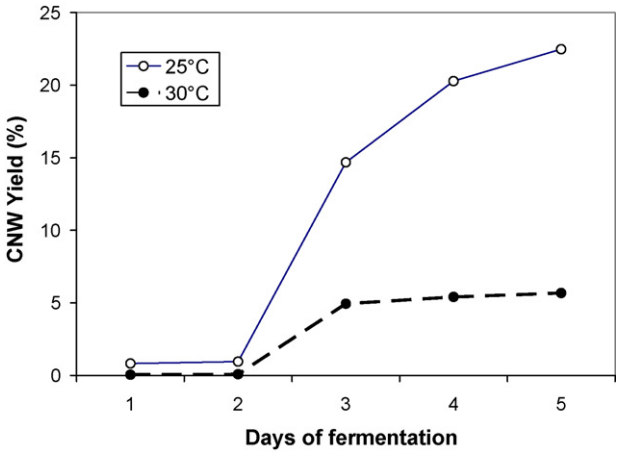

Fig. 1. Yield of CNW at two different temperatures of fermentation.

During submerged fermentation, the FPA (0.7 IU/ml), CMCase (0.07 IU/ml) and β-glucosidase (69.89 IU/ml) activities were found to reach their maxima at 5 days of incubation after which there was a significant drop in their activities. The direct dry weight estimation of fungal biomass was not possible since the fungal mycelium got entangled with the substrate. So the indirect method based on the glucosamine concentration was carried out for biomass determination. The glucosamine is one of the components present in the cell wall of fungi. The biomass concentration showed an increase for the initial 4 days after which there was no significant increase in the biomass concentration and growth of the fungus entered the stationary phase. The substrate concentration (initial MCC: 10 mg/ml) reduced drastically on the 1st day of fungal growth followed by a steady and slow decline. The amount of MCC was estimated to be 5.33, 4.53, 4.04, 3.42 and 3.20 mg/ml during 1–5 days of incubation, respectively.

The cellulose analysis by chemical method was used for the estimation of percent yield of CNW at different incubation periods. The yield of nanocellulose is given in Fig. 1. Till 2 days of fermentation, the yield was very low after which there was an exponential increase in the yield. The yield pattern corresponds to the growth pattern of the fungus. The maximum yield achieved was 22% while it was 51% in case of CNW prepared by acid hydrolysis. The comparatively low yield could be attributed to the fact that fungus is consuming significant amount of MCC for its growth and converted into biomass.

The fungal filtrate was collected and the protein was precipitated by saturated ammonium sulfate and re-suspended in acetate buffer. Electrophoresis of the protein was carried out to analyze the number of different sized fragments available in that mixture. Fig. 2 represents the stained gel showing bands corresponding to different protein fractions. The calibration was done by plotting linear regression curve for the standard protein markers using the Rf values. Table 1 shows the ten protein bands observed in our sample, out of which six bands could be identified and these values are well in line with the available literature values. (Beldman, Leeuwen, Rombouts, & Voragen, 1985; Li, Flora, & King, 1965; www.expasy.ch).

For particle size distribution, the suspended nanoparticles were diluted appropriately and analyzed in DLS particle size analyzer. The intensity of light scattered in a particular direction by dispersed particles tends to periodically change with time. These fluctuations in the intensity vs. time profile are caused by the constant changing of particle positions brought on by Brownian motion. DLS

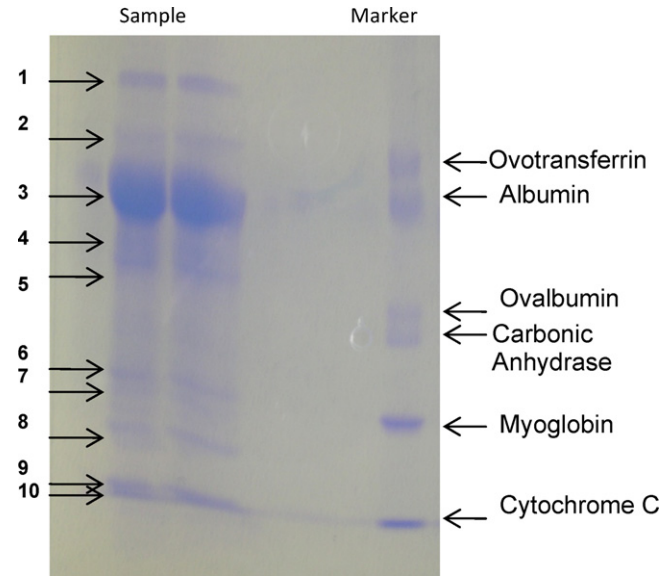

Fig. 2. Electrophoresis of extra cellular protein secreted by *T. reesei* during submerged state fermentation. First two lanes correspond to samples while the last lane represents the marker.

instruments obtain, from the intensity vs. time profile, a correlation function. This exponentially decaying correlation function is analyzed for characteristic decay times, which are related to diffusion coefficients and then by the Stokes–Einstein equation, to a particle radius. The percent composition of different sizes of CNW at an interval of 24 h is given in Fig. 3 while the particle size distribution is given in Fig. 4. The linearity in particle size reduction was not observed due to the fact that the process is a dynamic system and the fungus tends to consume the CNW formed initially.

The physical mechanism that is used to stabilize most aqueous nanoparticles systems is electrostatic repulsion. The colloidal particles of interest are charged, resulting in their mutual repulsion at extended distances. Ideally, the repulsive forces are sufficiently strong to prevent the particles from diffusing close to each other, where short-range van der Waals attractive forces dominate and lead to aggregation. Zeta potential is derived from measuring the mobility distribution of a dispersion of charged particles as they are subjected to an electric field. Mobility is defined as the velocity of a particle per electric field unit and is measured by applying an electric field to the dispersion of particles and measuring their average velocity. The Smoluchowski equation was used to obtain the zeta potential from the measured mobility. The cellulosic surfaces generally show bipolar character with prevalent acidic contribution due to the proton of the hydroxyl functional group as well as of present carboxyl groups. The average zeta potential of −21.73 and −15.57 mV were reported for bleached cotton and enzymatically treated cotton, respectively (Buschle-Diller, Inglesby, & Wu, 2005). In this study, the average zeta potential of CNW prepared by acid hydrolysis is −69.7 mV while that of microbial hydrolyzed is −14.6 mV. The high negative charge on the surface of CNW prepared by acid hydrolysis indicates the attachment of sulfate groups on its surface; though it gives more stability, eco-friendliness is lost here. The zeta potential of microbial prepared CNW was very close to that of pristine and enzymatically treated cotton as given in the literature (Buschle-Diller et al., 2005).

Table 1
Identification of protein bands separated by SDS-PAGE.

Bands	Identification[a]	Molecular weight (kDa)
1	α-Glucuronidase	91
2	β-Glucosidase	78
3	CBH-I & CBH-II	65
4	EG-I	48
5	EG-IV	32
6	EG-III	23
7	LMW Endoglucanase	19
8	Glycoprotein fragment of CBH-II	14
9	CBD	13
10	Fibril forming protein	12

[a] EG—endoglucanase; CBH—cellobiohydrolase; LMW—low molecular weight; CBD—cellulose binding domain.

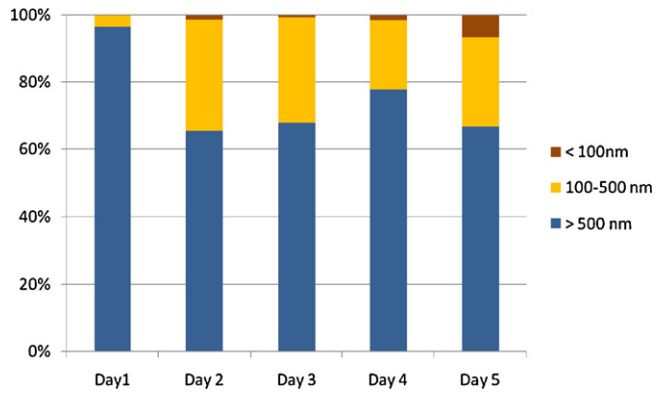

Fig. 3. Kinetics of cellulose particle size during 5 days of incubation as analyzed by DLS particle size analyzer.

The XRD analysis of MCC and CNW was done to determine the crystallinity, also called as degree of order, is the important aspect to understand the moisture sorption, swelling ability and accessibility to cellulase enzyme. XRD has been found to be sensitive to well-ordered regions in cellulose larger than 1.0 nm. Microfibrils are arranged into lattices within the cell wall: this result in a highly crystalline structure that is insoluble in water and resistant to reagents. However, areas of the lattice contain unstructured regions that are caused by the presence of amorphous cellulose, or which arise as a result of small crystalline units being imperfectly packed together. There is a marginal reduction in crystallinity in CNW prepared by acid hydrolysis while significant reduction (10%) was noticed in case of microbial prepared CNW. This is in contradiction to enzyme hydrolysis, where the crystallinity increases due to selective hydrolysis of amorphous region (Cao & Tan, 2002). In case of microbial hydrolysis, penetration of fungal mycelium into MCC might have contributed to the reduction in crystallinity.

Table 2 shows the DP values and crystallinity values of CNW as analyzed by XRD. The crystallite sizes match very well with the

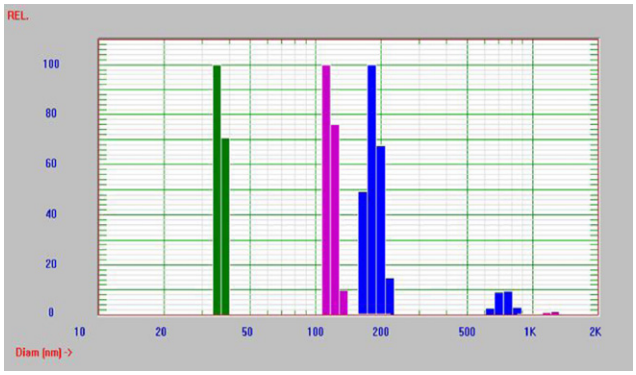

Fig. 4. Particle size distribution of CNW after 1 day (blue), 3 days (pink) and 5 days of hydrolysis (green) as analyzed by DLS particle size analyzer. (For interpretation of the references to colour in this figure legend, the reader is referred to the web version of the article.)

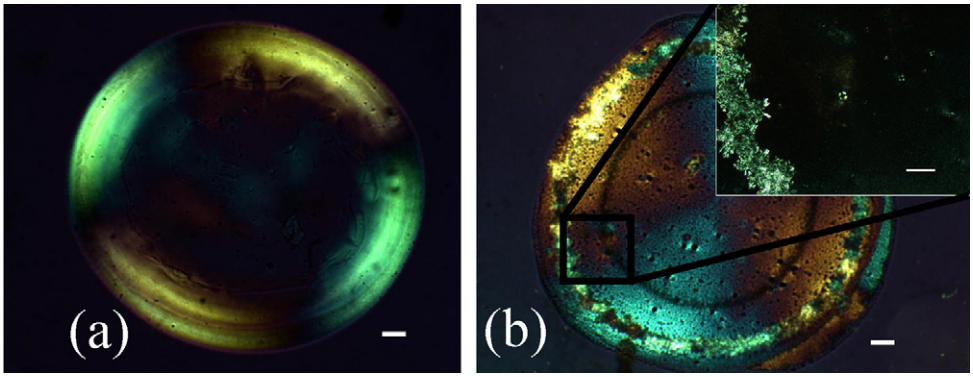

Fig. 5. Photomicrograph between crossed polarizers of dried CNW suspension prepared by acid hydrolysis (a) and by microbial hydrolysis (b). Inset in (b) shows the presence of polydomain under magnified view. Crossed polarizers are vertical and horizontal (scale bar 10 μm).

reported literature values (Patil, Dweltz, & Radhakrishnan, 1965). No significant change in crystallite size was observed in case of both acid and microbial hydrolyses as we did not reach that size of crystallites in preparation. The DP along the chains in native cellulose is very high, with values ranging from 2000 to 13,000 as claimed by some authors (Moharir, Van-Langenhove, Van-Nimmen, Louwagie, & Kiekens, 1999). During preparation of MCC itself, DP has reduced more than five times (to 465.7 ± 6.1) and further hydrolysis with acid resulted in DP by half (215.0 ± 1.0). During microbial hydrolysis, the DP has reduced gradually from day 1 to day 5, 401.1 ± 3.3, 368.7 ± 6.8, 344.4 ± 1.9, 297.5 ± 0.6 and 293.0 ± 0.8, respectively. Since the initial hydrolysis does not significantly reduce the DP, the yield of CNW was low during that period as shown in Fig. 1.

The suspension of CNW displays liquid crystalline behaviour above a critical concentration, due to their rod-like shape in agreement with Onsager's theory for rigid rod-like particles (Onsager, 1949). At low CNW concentration the suspensions are isotropic, with a random arrangement, while at high concentration, the suspensions are anisotropic, with the CNW packed in a chiral nematic arrangement (Edgar & Gray, 2002). In polarized light microscopy (PLM), the interference colours are generated in birefringent specimens in transmitted white light between two polarizers whose vibrational directions are at 90°. The plane polarized light on passing through the nanocellulose with its optical axis perpendicular to the direction of light propagation, is split into slow ray and fast ray. The retardation of both these rays generates a phase difference as they emerge from the sample. These two rays are recombined into a single ray as they pass through the second polarizer, and they interfere either destructively or constructively depending on the phase difference introduced by the birefringent nanocellulose. A precise hue of interference colour will be generated depending on the relative retardation (of the slow vs. the fast ray) (Ross et al., 1997).

Cellulose nanocrystals dispersed in water form a stable chiral nematic liquid crystal phase above a critical concentration (Revol, Bradford, Giasson, Marcessault, & Gray, 1992). The self-assembly of chiral nematic phases by suspensions of cellulose crystallites has received an increasing amount of attention for its potential applications. Alignment of nanofillers in a polymer helps to obtain a unidirectional reinforced nanocomposite with improved mechanical strength in the aligned direction. Suspensions of cellulose nanocrystals are often stabilized by negative surface charges from carboxyl or sulfate ester groups on their surface. Cranston and Gray (2006) reported no orientation of cellulose nanocrystals prepared by acid hydrolysis when 9% nanocrystal suspension was dried on poly(allyl) amine hydrochloride coated silicon wafer and chiral nematic structure when an external magnetic field is applied. By simply casting films from suspensions of cellulose crystallites, cellulose films with the optical properties of chiral nematic liquid crystals can also be prepared. Tailoring of the films to give different colours of reflected light was achieved by altering the salt content of the suspension for a given source of cellulose and set of hydrolysis conditions. Possible areas of application include optically variable films and inks for security papers.

In this study, we could demonstrate two different alignments of CNW prepared by two different processes. In contrast to earlier studies where polydomain structure with the helical axes of different chiral nematic domains pointing in different directions were reported, we have achieved a monodomain in case of CNW prepared by acid hydrolysis due to long-range uniform orientation when a drop of 5 μl is allowed to dry on the surface of glass slide (Fig. 5a). In case of CNW prepared by microbial process, apart from long-range orientation, polydomain was observed due to many short-range orientations (Fig. 5b). This could be due to the very low zeta potential of CNW prepared by microbial hydrolysis process in compared to that of acid hydrolyzed. A full-wave retardation plate was inserted into the optical path of the microscope to identify the local orientation. With a full-wave retardation plate, a blue colour appears where the slow axis of the birefringent sample is aligned with the slow axis of the wave plate and a yellow colour

Table 2
DP and crystallinity analysis of CNW with size analysis of CNW by DLS size analyzer and AFM.

Samples	Degree of polymerization (DP)	XRD				Size		
		Crystallinity (%)	Crystallite size (nm)			DLS particle size analysis	AFM analysis	
			(002)	(101)	(10$\bar{1}$)		Length	Thickness
CNW prepared by acid hydrolysis	215.0 ± 1.0	86.42	6.3	4.2	5.0	53.5 ± 5.3	287.24 ± 79.75	29.69 ± 5.07
CNW prepared by microbial hydrolysis	293.0 ± 0.8	78.39	6.3	4.2	4.3	36.5 ± 1.9 nm	120.27 ± 36.25	40.74 ± 7.59
MCC	465.7 ± 6.1	88.26	6.3	4.4	5.0	45–53 μm (by sieving process)		

appears where the fast axis of the sample is aligned with the slow axis of the wave plate. Crystalline cellulose is optically biaxial. The slow axis, in the direction of largest refractive index, is oriented along the cellulose backbone and thus along the long axis of the nanocrystals. As a result of parallel arrangement of CNW in chiral nematic phase, each nematic plane has a slow axis in the direction of the nematic director and a fast axis perpendicular to it.

Tapping mode AFM, employing a silicon nitride cantilever probe to gently oscillate and tap the sample surface, is very well suitable for organic materials like CNW at low forces. The cantilever is excited into its resonance oscillation and the sample surface will be scanned. Fig. 6 shows the tapping mode AFM images of CNW prepared by acid hydrolysis (a) and by microbial hydrolysis (b and c). The size of short-range orientation as observed in Fig. 6c very well corroborated with that of photomicrograph observed with crossed polarizers. The image CNW prepared by acid hydrolysis showed a well separated distribution due to the sulfation of its surfaces; while in case of CNW prepared by microbial hydrolysis, aggregates were noticed. The length and thickness of CNW were analyzed from the AFM images using the ImageJ™ software and given in Table 2. The CNW prepared by acid hydrolysis was narrow and sharper leading to high aspect ratio while that of microbial prepared CNW had low aspect ratio. This resultant shape could be due to differences in the mode of action by acid and fungus. Since acid hydrolysis is completely a surface phenomenon, its action is influenced purely by crystallite size and shaking condition resulting in high aspect ratio. In case of microbial hydrolysis, apart from shaking condition, two other parameters that influence the resultant shape of CNW are: effect of cellulose binding domain secreted by the fungus in loosening up the crystalline structure and the penetration of mycelium into the MCC. This result is supported by reduction in crystallinity as analyzed by XRD.

Fig. 7 shows the FTIR spectra of CNW and pristine cotton cellulose. The characteristic peaks for cellulose (Oh, Yoo, Shin, & Seo, 2005) are the hydrogen-bonded stretching at 3344 cm^{-1}, the OH bending of the adsorbed water at 1646 cm^{-1}, the CH stretching at 2900 cm^{-1}, the HCH and OCH in-plane bending vibrations at 1432 cm^{-1}, the CH deformation vibration at 1373 cm^{-1}, the COC, CCO, and CCH deformation modes and stretching vibrations in which the motions of the C-5 and C-6 atoms are at 898 cm^{-1}, and the C–OH out-of-plane bending mode around 670 cm^{-1}. These peaks match well in both the spectra and no significant difference could be observed, suggesting the unaltered surface chemistry of CNW prepared by microbial hydrolysis.

Apart from use in composites, CNW find applications in health care like personal hygiene products, biomedicines, cosmetics etc (Ioelovich & Leykin, 2004). CNW in its pure form is safe and biocompatible; but the traditional acid hydrolysis process inserts sulfate groups on the surface of CNW. Earlier report revealed sulfur content of 0.73% (w/w) which suggests sulfur deposition on the surface of CNW as a result of side reaction during hydrolysis (Fleming, Gray, & Matthews, 2001). While these surface modifications pose bio-compatibility problems, fungal degraded cellulose retains its original chemical nature. Cellulase enzyme produced by various microbes, with its proven biotechnological advances in various fields (Ioelovich, 2008; Bhat, 2000), will be of immense use in the production of CNW. The use of biodegradable materials like polylactic acid (PLA), polyhydroxy alkanoates (PHAs), cellulosic plastics, starch and soy protein plastics are very much restricted due to the problem of low strength and high vapour permeability. Use of CNW as fillers in biodegradable polymers permits both increase in mechanical strength, acceleration in the rate of biodegradation (Ohmiya, Sakka, Karita, & Kimura, 1997) and reduce the vapour permeability. So, biologically prepared CNW will prove to be of immense use in various eco-friendly applications.

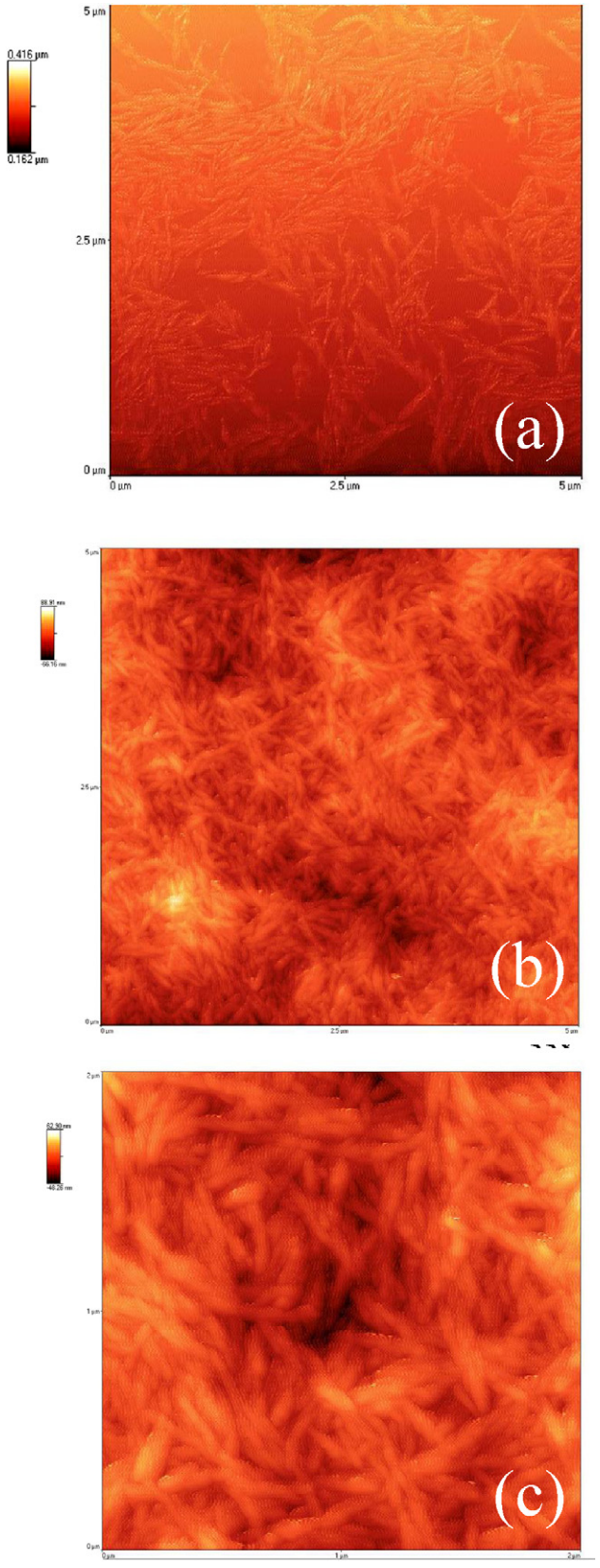

Fig. 6. AFM images of the CNW prepared by acid (a) and microbial (b, c) hydrolysis.

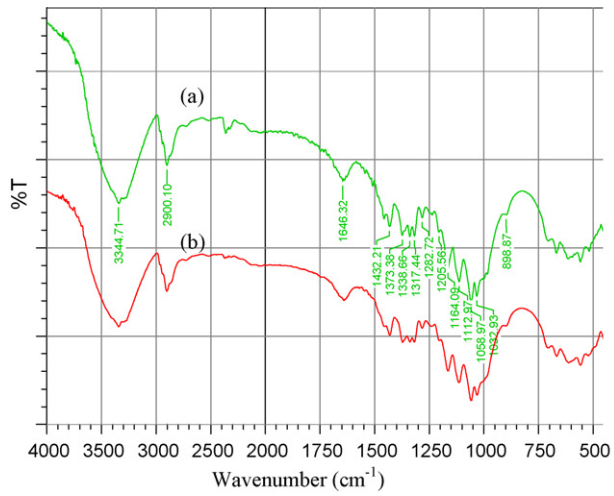

Fig. 7. FTIR spectra of CNW prepared by microbial hydrolysis (a) and that of pristine cotton (b).

4. Conclusions

Isolation methods of CNW are expanding rapidly due to its promising mechanical properties, biodegradability and eco-friendliness. In this work, we have explored a possibility of controlled hydrolysis of MCC using the fungus *T. reesei* with the yield potential of 22%. The penetration of fungus into the ordered regions of MCC during incubation resulted in reduced crystallinity of CNW prepared by microbial hydrolysis compared to that of acid hydrolysis. The reinforcing effect of CNW in polymer composites is mainly due to very strong and rigid three-dimensional network of hydrogen-bonded whiskers. The traditional method of acid hydrolysis resulted in sulfation on the surface of CNW while the surface chemistry of CNW prepared by fungal hydrolysis remains unaltered; this in turn will improve its performance as nanofillers in composites. Also, this enhances the bio-compatibility of CNW and its scope in biomedical applications and pharmaceuticals.

Acknowledgements

The authors are thankful to Dr. S. Sreenivasan, Director Central Institute for Research on Cotton Technology for his kind suggestion and support for this research work. We gratefully acknowledge the technical support rendered by Mr. Vivekanandan and Mr. Sekar in carrying out the experiments. This research was supported by the National Agricultural Innovation Project (NAIP), Indian Council of Agricultural Research (ICAR) through its sub-project entitled 'Synthesis and characterization of CNW and its application in biodegradable polymer composites to enhance their performance', code number 'C2041'.

References

Abd-Aziz, S., Hung, G. S., Hassan, M. A., Karim, M. I. A., & Samat, N. (2008). Indirect method for quantification of cell biomass during solid state fermentation of palm kernel cake. *Asian Journal of Scientific Research*, *1*(4), 385–393.

Araki, J., Wada, M., Kuga, S., & Okana, T. (1998). Influence of dope solvents on physical properties of wet-spun cellulose. *Colloids and Surfaces A*, *42*(1), 75–82.

Bai, W., Holbery, J., & Li, K. (2009). A technique for production of nanocrystalline cellulose with a narrow size distribution. *Cellulose*, *26*, 455–465.

Barbagallo, R. N., Spagna, G., Palmeri, R., Restuccia, C., & Giudici, P. (2004). Selection, characterization and comparison of β-glucosidase from mould and yeasts employable for enological applications. *Enzyme Microb Technol*, *35*, 58–66.

Beldman, G., Leeuwen, M. S., Rombouts, F., & Voragen, F. (1985). The cellulase of *Trichoderma viride*. *European Journal of Biochemistry*, *146*, 301–308.

Bhat, M. K., & Bhat, S. (1997). Cellulose degrading enzymes and their potential industrial applications. *Biotechnological Advances*, *15*(3–4), 583–620.

Bhat, M. K. (2000). Cellulases and related enzymes in biotechnology. *Biotechnological Advances*, *18*(5), 355–383.

Buschle-Diller, G., Inglesby, M. K., & Wu, Y. (2005). Physicochemical properties of chemically and enzymatically modified cellulosic surfaces. *Colloids and Surfaces A: Physicochemical Engineering Aspects*, *260*, 63–70.

Cao, N. J., Xia, Y. K., Gong, C. S., & Tsao, G. T. (1997). Production of 2,3-butanediol from pretreated corn cob by *Klebsiella oxytoca* in the presence of fungal cellulase. *Applied Biochemistry and Biotechnology*, *63*, 129–139.

Cao, Y., & Tan, H. (2002). Effects of cellulase on the modification of cellulose. *Carbohydrate Research*, *337*, 1291–1296.

Charlet, G., & Gray, D. G. (1987). Solid cholesteric films cast from aqueous (hydroxypropyl) cellulose. *Macromolecules*, *20*(*1*), 33–38.

Cranston, E. D., & Gray, D. G. (2006). Formation of cellulose-based electrostatic layer-by-layer films in magnetic field. *Science and Technology of Advanced Materials*, *7*, 319–321.

Edgar, C. E., & Gray, D. G. (2002). Acid hydrolysis of cellulose fibers produces suspensions of colloidal cellulose nanocrystals. *Macromolecules*, *35*, 7400–7406.

Elson, L. A., & Morgan, W. (1933). A colorimetric method for the determination of glucosamine and chondrosamine. *Biochemical Journal*, *27*, 1824–1828.

Filson, P. B., & Dawson-Andoh, B. (2009). Sono-chemical preparation of cellulose nanocrystals from lignocellulose derived materials. *Bioresource Technology*, *100*, 2259–2264.

Fleming, V., Gray, D. G., & Matthews, S. (2001). Cellulose crystallites. *Chemistry European Journal*, *7*(9), 1831–1835.

Ghose, T. K. (1987). Measurement of cellulase activities. *Pure and Applied Chemistry*, *59*, 257–268.

Grobe, A. (1989). Chapter V. In J. Brandrup, & E. H. Immergut (Eds.), *Polymer handbook*. New York: John Wiley & Sons.

Hayashi, N., Kondo, T., & Ishihara, M. (2005). Enzymatically produced nano-ordered short elements containing cellulose I_β crystalline domains. *Carbohydrate Polymers*, *61*, 191–197.

Hayashi, N., Sugiyama, J., Okano, T., & Ishihara, M. (1997). The enzymatic susceptibility of cellulose microfibrils of the algal–bacterial type and the cotton–ramie type. *Carbohydrate Research*, *305*, 261–269.

Ioelovich, M., & Leykin, V. (2004). Nano-cellulose and its application. *Journal of SITA*, *6*(*3*), 17–24.

Ioelovich, M. (2008). Cellulose as a nanostructured polymer: A short review. *BioResources*, *3*(4), 1403–1418.

Janardhnan, S., & Sain, M. M. (2006). Isolation of cellulose microfibrils—An enzymatic approach. *BioResources*, *1*(2), 176–188.

Kleinebudde, P., Jumaa, M., & El Saleh, R. (2000). Direct pelletization in a rotary processor controlled by torque measurements. II. Effects of changes in the content of microcrystalline cellulose. *AAPS PharmSci*, *2*(3), 5–10.

Lee, S. Y., Mohan, D. J., Kang, I. A., Doh, G. H., Lee, S., & Han, S. O. (2009). Nanocellulose reinforced PVA composite films: Effects of acid treatment and filler loading. *Fibres and Polymers*, *10*(1), 77–82.

Li, L., Flora, R., & King, K. (1965). Individual roles of cellulase components derived from *Trichoderma viride*. *Archives of Biochemistry and Biophysics*, *111*, 439–447.

Luo, J., Xia, L. M., Lin, J. P., & Cen, P. L. (1997). Kinetics of simultaneous saccharification and lactic acid fermentation processes. *Biotechnology Progress*, *13*, 762–767.

Moharir, A. V., Van-Langenhove, L., Van-Nimmen, E., Louwagie, J., & Kiekens, P. (1999). Stability of X-ray cellulose crystallite orientation: Parameters in native cotton with change of location and year of growth. *Journal of Applied Polymer Science*, *72*, 269–276.

Nelson, N. (1944). A photometric adaptation of the Somogyi method for the determination of glucose. *Journal of Biological Chemistry*, *153*, 375–380.

Nishino, T., Takano, K., & Nakamae, K. J. (1995). Elastic modulus of the crystalline regions of cellulose polymorphs. *Journal of Polymer Science Part B: Polymer Physics*, *33*(11), 1647–1651.

Oh, S. Y., Yoo, D. I., Shin, Y., & Seo, G. (2005). FTIR analysis of cellulose treated with sodium hydroxide and carbon dioxide. *Carbohydrate Research*, *340*, 417–428.

Ohmiya, K., Sakka, K., Karita, S., & Kimura, T. (1997). Structure of cellulases and their application. *Biotechnology and Genetic Engineering Reviews*, *14*, 365–414.

Olsson, L., & Hahn-Hagerdahl, B. (1996). Fermentation of lignocellulosic hydrolysates for ethanol production. *Enzyme and Microbial Technology*, *18*, 312–331.

Onsager, L. (1949). The effects of shape on the interaction of colloidal particles. *Annals of the New York Academy of Sciences*, *51*, 627–659.

Paralikar, K. M., & Bhatawdekar, S. P. (1983). Hydrolysis of cotton fibers by cellulase enzyme. *Journal of Applied Polymer Science*, *29*(*8*), 2573–2580.

Patil, N. B., Dweltz, N. E., & Radhakrishnan, T. (1965). Studies on decrystallization of cotton. *Textile Research Journal*, *35*, 517–523.

Revol, J.-F., Bradford, H., Giasson, J., Marcessault, R. H., & Gray, D. G. (1992). Helicoidal self-ordering of cellulose microfibrils in aqueous suspension. *International Journal of Biological Macromolecules*, *14*(3), 170–172.

Revol, J. F., Dietrich, A., & Goring, D. A. I. (1987). Effect of mercerization on the crystallite size and crystallinity index in cellulose from different sources. *Canadian Journal of Chemistry*, *65*, 1724–1725.

Ross, S., Newton, R., Zhow, Y. M., Haffegee, J., Ho, M. –W., Bolton, J. P., et al. (1997). Quantitative image analysis of birefringent biological material. *Journal of Microscopy*, *187*, 62–67.

Sturcov, A., Davies, G. R., & Eichhorn, S. J. (2005). Elastic modulus and stress-transfer properties of tunicate cellulose whiskers. *Biomacromolecules*, *6*, 1055–1061.

Updegraff, D. M. (1969). Semi microdetermination of cellulose in biological materials. *Analytical Biochemistry*, *32*, 420–429.

Vigneshwaran, N., & Kathe, A. A. (2009). *Indian patent application no. 3012/MUM/2009*, pp. 1–8

Weber, K., & Osborn, M. (1969). The reliability of molecular weight determinations by dodecyl sulfate-polyacrylamide gel electrophoresis. *Journal of Biological Chemistry*, *244*, 4406–4412.

Zaldivr, M., Velasquez, J. C., Contreras, I., & Perez, L. M. (2001). *Trichoderma aureoviride* 7–121, a mutant with enhanced production of lytic enzymes: Its potential use in waste cellulose degradation and/or biocontrol agent. *Electronic Journal of Biotechnology*, *4*(3), 1–7.